Refractivity and Refractivity Gradient Estimation from Radar Phase Data: A Least Squares Based Approach

Rubén Nocelo López, Brais Sánchez-Rama, Verónica Santalla del Río, *Member, IEEE,* Sérgio Barbosa, Paulo Narciso, Román Pérez-Santalla, Alberto Pettazzi, Paulo Pinto, Santiago Salsón and Tânia Viegas

***Abstract*—Tropospheric refractivity, related to temperature, pressure and humidity is an interesting parameter for weather analysis, prediction and study of climate trends. It has been shown to be useful for the detection and forecast of convective events. It has already been demonstrated that tropospheric refractivity can be estimated from radar phase measurements. In this paper a non-linear least squares based approach for the estimation of the tropospheric refractivity that simultaneously provides estimates of the refractivity vertical gradient is presented. A significant improvement of the presented technique is that it allows estimation of the refractivity over any terrain orography, flat or hilly. Furthermore, the method developed can be implemented on klystron as well as on magnetron based radars. Results for both radar types, at S- and C-band, located over flat and hilly terrain show the potential of the method.**

***Index Terms*—Atmospheric refractivity, least squares estimation, radar.**

I. Introduction

THE relationship of tropospheric refractivity with temperature, pressure and humidity has made it an interesting parameter for weather diagnosis and forecasting, as well as for climate analysis. Since the late 1990's, the Radio Occultation (RO) technique has been implemented to measure the refractivity of the Earth's atmosphere, [1], [2]. Early experiments have already demonstrated that the refractivity data obtained by RO could significantly contribute to improve the forecasting performance of Numerical Weather Prediction (NWP) models. Nowadays the benefits of RO refractivity data are indisputable. The RO refractivity data possess very interesting features such as high precision and accuracy, high vertical resolution and global coverage. On the other hand, precision and accuracy decrease as height decreases and data for the lower troposphere are scarce, specially in areas with rugged orography.

Based on the demonstrated utility of refractivity data, another approach to measure refractivity in the lower troposphere was proposed in [3]. This technique considers obtaining the refractivity from the phase of radar signals backscattered from stationary ground targets. Initial results were promising, encouraging the research and development of the technique while large experiments were planned and conducted to evaluate the performance and potential of radar refractivity measurements. The IHOP_2002 experiment conducted in the Oklahoma Panhandle was designed to obtain refractivity measurements with different sensors/instruments: weather stations, mobile mesonets, aircraft in-situ, AERI (Atmospheric Emitted Radiance Interferometer), radiosondes and the National Center for Atmospheric Research (NCAR) S-Pol radar. Intercomparisons between radar refractivity measurements and refractivity measurements obtained with the other instruments showed a high correlation between them. Additionally, it was found that radar refractivity may help in the detection of boundary layer convergence zones and forecasting of convective initiation in [4]. Later, the Refractivity Experiment for H_20 Research and Collaborative Operational Technology Transfer (REFRACTT) took place in Northeastern Colorado between June 2006 and August 2006. Research and operational radars (NCAR S-Pol, CSU-CHILL and NEXRAD) were used for this experiment. Refractivity fields over a large area were obtained, the relationship of the refractivity temporal and spatial variability to the temporal and spatial variability of water vapour and the initiation of convection processes was again shown in [5]. Refractivity retrieval from phase measurements obtained with the National Weather Radar Testbed phased array radar and the US operational radar network, both at S-band, was also demonstrated by [6].

Radars used in these experiments were coherent systems, based on klystron transmitters. Implementation of the radar refractivity estimation technique with magnetron-based radars was challenging. In [7], [8] and [9] the errors caused by the frequency drifts of magnetron-based radars were described and analysed. Since most European weather radars use magnetron transmitters, it was necessary to modify the radar refractivity estimation technique for its implementation in Europe. Subsequent refractivity measurements obtained with

Manuscript received April XX, 2022; revised XX YY, 2022.

This work was supported in part by the LIFE Program of the European Union (Project Life16 Env/ES/000559, LifeTEC) and in part by Xunta de Galicia under Grant GRC2019/026. (*Corresponding author: Verónica Santalla del Río.*)

R. Nocelo López, B. Sánchez-Rama and V. Santalla del Río are with the atlanTTic Research Center, Universidade de Vigo, 36310 Vigo, Spain. (e-mail: veronica@uvigo.es).

S. Barbosa, P. Narciso, P. Pinto and T. Viegas are with the Portuguese Institute for Sea and Atmosphere (IPMA), 1749-077 Lisboa, Portugal.

A. Pettazzi and S. Salsón are with MeteoGalicia, Xunta de Galicia, 15707 Santiago de Compostela, Spain.

magnetron based radars, e.g. during the HyMeX campaign in the southeast part of France, showed good correlation with weather station measurements in [10].

The potential of this radar refractivity technique and its current problems were discussed in [11], [12], [7]. Important features of the radar refractivity estimation technique are its high temporal and spatial resolutions, though the area covered by each radar is relatively small, 30 to 50 km in range [13]. The use of not only weather radar networks, but also other civil radar networks can help to increase the coverage. Then, assimilation of radar refractivity data into NWP models can improve the prediction of storm initiation [14], [15], [16].

On the other hand, an important limitation of the current technique is that the height difference between stationary targets and between them and the radar is not taken into account. In relatively flat areas, with small height differences, the error in the final refractivity estimates due to height differences between the targets and the radar is relatively small. As the difference between the height of the targets and the height of the radar increases the error increases beyond acceptable values. Therefore, the deployment of the radar-based refractivity estimation technique is limited to flat areas. Correcting the error in the refractivity estimates caused by the different height of the targets and the radar requires knowledge of the refractivity vertical gradient. Different approaches to obtain the refractivity gradient have been proposed [17], [18], [19]. Those presented in [17] and [18] are based on power measurements. The method for refractivity gradient estimation presented in [17] is based on the comparison of the ground echo map measured with estimated ground echo maps for different refractivity gradient values. The method was tested with data obtained during the IHOP_2002 experiment. The method showed, as stated by the authors, "an ability in capturing the near ground gradient of refractivity at low level elevation angles". However, the accuracy of some results was seriously affected by precipitation outflows. In general, results will worsen as the scattering properties of the ground targets change with time and climatological conditions. Moreover, the tests were conducted with data obtained over a flat area. In hillier areas, the orography might be the principal factor that determines the ground echo maps, making difficult the implementation of the method proposed. The method proposed in [18] is based on the linear relationship between the returned power variation with the elevation angle and the refractivity gradient. Though the refractivity gradient estimates obtained with this method correlate well with refractivity gradient measurements from other instruments, they present significant biases. These are caused by small biases of the antenna elevation pointing angle, fluctuations of the returned power and errors in the estimated target heights that will increase in a rougher orography. On the other hand, the approach presented in [19] is based on phase measurements. It considers joint estimation of the refractivity and the refractivity gradient from radar phase measurements. The results were encouraging though the method required to be recalibrated every few days, making difficult its implementation in operational radars.

Therefore, there is still a need for a method to estimate the refractivity at a given height and the refractivity gradient while it can be implemented in operational radars working on either flat or hilly areas. Departing from the phase variation of radar returned signals due to changes of the refractivity and its vertical gradient [17], [19], the refractivity estimation algorithm proposed in [19] is reformulated considering that it must work with klystron and magnetron operational radars, located either in flat or hilly areas. For an operational use of the algorithm it is also required to reduce the frequent recalibration demanded by the algorithm as initially proposed in [19].

Section II briefly reviews the previous work on radar refractivity estimates and Section III describes the least squares based approach proposed in this paper for the estimation of the refractivity at the radar height and its gradient. Finally, Sections IV and V discuss the algorithm implementation and the achieved results respectively.

II. Estimation of the Refractivity and its Gradient: Previous work

Radar refractivity estimation is based on the variation of the phase of backscattered pulses from stationary targets with the troposphere refractive index. Let us consider a stationary target $T0$. Assuming a spherically stratified troposphere where the index of refraction linearly decreases with height [20], the phase of the m-th backscattered pulse from the stationary target $T0$, the target $T0$ phase, is given by [12], [19]:

$$\Phi_{T0}(m) = -2\pi f_{LO}\left[\frac{k_{T0}2\Delta R'}{c}\right] + \phi_{T0} - 2\pi(f_c + f_{LO}) \cdot \left[\frac{\delta_{T0}(m)}{c} + \frac{L_{T0}(m)}{c} + \frac{L_{C0}(m)}{c}\right] + \phi_{T0}^{CT}(m) \quad (1)$$

with

- f_c is the actual transmitter frequency.
- f_{LO} is the sum of all the frequencies of the different downconversion stages, corresponding to the expected frequency of the transmit pulse.
- $L_{T0}(m) = R_{T0}\left(\overline{N}(m)\cdot 10^{-6} + \frac{h_{T0}-h_R}{2}\frac{\partial N(m)}{\partial h}\cdot 10^{-9}\right)$
- $L_{C0}(m) = \frac{R_{T0}(h_{T0}-h_R)^2 - R_{T0}^3}{12a_e}\frac{\partial N(m)}{\partial h}\cdot 10^{-9}$
- $\overline{N}(m)$ the mean refractivity at the radar height.
- $\frac{\partial N(m)}{\partial h}$ the refractivity gradient per km.
- R_{T0} the length of the ray path to the target, $R_{T0} = k_{T0}\Delta R' + \delta_{T0}(m)$ with $k_{T0}\Delta R'$ being the distance to the center of the range gate where the target is located and $\delta_{T0}(m)$ being the distance between the target and the range gate center at the transmission of the m-th pulse.
- h_{T0} the target $T0$ height.
- h_R is the radar height.
- a_e the modified Earth's radius [20].
- ϕ_{T0} the stationary target backscattering phase.
- $\phi_{T0}^{CT}(m)$ the clutter contribution to the phase. It is modelled as a zero mean random variable that adds to the stationary target phase.

The main steps and assumptions considered for obtaining the target $T0$ phase are summarized in the Appendix.

Equation (1) shows the relationship between the target $T0$ phase and the mean refractivity and its gradient. Unfortunately, the rapid wrapping of this phase with distance and the

unknown stationary target backscattering phase, ϕ_{T0}, makes impossible to obtain the mean refractivity and its gradient from single target measurements. However, if changes of the refractivity and/or its gradient are small enough, the absolute change in the target $T0$ phase is below 180^o. Then, measurement of the target $T0$ phase change may allow to estimate changes in the troposphere refractivity conditions according to [3]. In order to do so, most works to date assumed "strictly flat earth", [11], that is, all targets are at the radar height and there are no changes of the refractivity gradient, so that, the target $T0$ phase change w.r.t. time, that is, between transmitted pulses m_1 and m_2, becomes:

$$\Delta\Phi_{T0}(m_1,m_2) = \\ -\frac{2\pi}{c}(f_c+f_{L0})R_{T0}\Delta\overline{N}\cdot 10^{-6}+\phi_{T0}^{CT}(m_2)-\phi_{T0}^{CT}(m_1) \tag{2}$$

which clearly allows to estimate $\Delta\overline{N} = \overline{N}(m_2) - \overline{N}(m_1)$ from the measurement of the phase change. To have unbiased estimates of $\Delta\overline{N}$ the phase change should be within $\pm 180^o$. Besides, it must be considered that, since $\Delta\Phi_{T0}(m_1,m_2)$ increases linearly with R_{T0}, the maximum distance from the target to the radar that ensures that $\Delta\Phi_{T0}(m_1,m_2)$ is within $\pm 180^o$, for a given value of $\Delta\overline{N}$, is a few km, decreasing as the radar frequency increases. The trade-off between the different parameters is well known [11], [21]. Table I summarizes some results for the S- and C- bands.

TABLE I
MAXIMUM DISTANCE TO A STATIONARY TARGET $T0$ TO ENSURE NO WRAPPING OF $\Delta\Phi_{T0}(m_1,m_2)$, CONSIDERING NO CLUTTER PHASE NOISE, FOR DIFFERENT VALUES OF $\Delta\overline{N}$.

Frequency Band	$\boldsymbol{\Delta\overline{N}=10}$	$\boldsymbol{\Delta\overline{N}=20}$	$\boldsymbol{\Delta\overline{N}=40}$
S-band	$\approx$ 2.70 km	$\approx$ 1.35 km	$\approx$ 0.70 km
C-band	$\approx$ 1.35 km	$\approx$ 0.70 km	$\approx$ 0.35 km

To increase the radar coverage for refractivity estimation, it was proposed in [11] to consider the change with time of the phase difference from two targets, e.g. $T0$ and $T1$, $\Delta\Phi_{T0,T1}(m) = \Phi_{T1}(m) - \Phi_{T0}(m)$.

Then, the phase difference change between transmitted pulses m_1 and m_2, considering the "strictly flat earth" approach and no changes in the refractivity gradient, is given by:

$$\Delta\Phi_{T0,T1}(m_1,m_2) = \Delta\Phi_{T0,T1}(m_2) - \Delta\Phi_{T0,T1}(m_1) = \\ \frac{2\pi}{c}(f_c+f_{L0})(R_{T0}-R_{T1})\Delta\overline{N}\cdot 10^{-6}+\phi_{T1}^{CT}(m_2) \\ -\phi_{T0}^{CT}(m_2)-\phi_{T1}^{CT}(m_1)+\phi_{T0}^{CT}(m_1) \tag{3}$$

The similarity between Equation (2) and (3) is obvious. Now, to avoid phase wrapping, it is $\Delta\Phi_{T0,T1}(m_1,m_2)$ what needs to be within $\pm 180^o$ for the maximum value of $\Delta\overline{N}$. That is, the distance between the targets $T0$ and $T1$ must be below a few hundred meters (see Table II), no matter what the distance from the radar to any of the targets is. Therefore, as far as the distance between the targets $T0$ and $T1$ does not grow up to cause wrapping, if the targets are located within the radar coverage area, Equation (3) can be used to calculate the refractivity. Evidently, the increase of the coverage comes at the expense of the increase in the clutter noise.

TABLE II
MAXIMUM DISTANCE BETWEEN TARGETS $T0$ AND $T1$ TO ENSURE NO WRAPPING OF $\Delta\Phi_{T0,T1}(m_1,m_2)$, CONSIDERING NO CLUTTER PHASE NOISE, FOR DIFFERENT VALUES OF $\Delta\overline{N}$.

Frequency Band	$\boldsymbol{\Delta\overline{N}=10}$	$\boldsymbol{\Delta\overline{N}=20}$	$\boldsymbol{\Delta\overline{N}=40}$
S-band	$\approx$ 2.70 km	$\approx$ 1.35 km	$\approx$ 0.70 km
C-band	$\approx$ 1.35 km	$\approx$ 0.70 km	$\approx$ 0.35 km

Either Equation (2) or Equation (3) allow to estimate just the refractivity change between the transmission of two pulses. The potential of refractivity change measurements has been discussed in [22]. However, the parameter of most interest is the absolute refractivity. To obtain the absolute refractivity it is necessary to know the absolute refractivity at the transmission of a first reference pulse. Then, two approaches may be considered. The absolute refractivity can be obtained either by accumulating the refractivity changes obtained from comparing the received phases of consecutive pulses transmitted just after the first reference pulse or by measuring the refractivity change of each transmitted pulse with respect to the first pulse. If the first approach is implemented [19], [22], the phase noise of the consecutive measurements accumulates so that the error of the measured absolute refractivity increases with the number of pulses transmitted after the reference pulse. To ensure the error of the absolute refractivity is within preset limits, recalibration, that is, measuring the absolute refractivity at the transmission of a new reference pulse would be required rather frequently as in [19], [22].

Now, regarding to the second approach [11], as the time of transmission of the current pulse w.r.t. the transmission of the reference pulse increases, the refractivity change increases and wrapping may happen. That is, for a given distance to the stationary target $T0$ if Equation (2) is used, or for a given distance between the targets $T0$ and $T1$ if Equation (3) is used, there is a maximum value of the refractivity change that may be measured. Let us put it another way, to ensure correct measurement of the highest refractivity change that may happen at a given location, the maximum distance to the stationary target or the maximum distance between the targets $T0$ and $T1$, has to be reduced (see Tables I and II).

Besides, for the implementation of this approach, the reference pulse and the corresponding absolute refractivity have to be established. The reference pulse phase (or the reference pulse phase difference) and the corresponding absolute refractivity are determined by averaging, to reduce the noise due to the clutter, the phases (or phase differences) received during a short period of time in which it can be assumed a homogeneous refractivity field in the area of interest [11].

Additionally, to reduce the noise, mainly due to the clutter, the refractivity measurements obtained from the backscattered phase of all stationary targets or target pairs, within an area where the refractivity can be considered statistically homogeneous, are somehow averaged as in [11], [4], [5], [10].

Besides the clutter noise, other sources of error have been identified and discussed in [11], [7]. Not accounting for the real height of the stationary targets is one of them, specially if there is a significant change of the refractivity gradient between the reference pulse and the received pulse. The error due to not considering the height of the stationary targets increases as the height difference between the targets and the radar increases, leading to useless results in non-flat areas.

Thus, in [19] the case when the "strictly flat earth" assumption cannot be considered and changes of the refractivity gradient need to be taken into account was studied. In this case the phase difference is given by:

$$\begin{aligned}\Delta\Phi_{T0,T1}(m) = -\frac{2\pi}{c} f_{LO}(k_{T1}-k_{T0})2\Delta R' + \\ \frac{2\pi(f_c+f_{L0})}{c}\big[(\delta_{T0}(m)-\delta_{T1}(m)) + \\ (L_{T0}(m)-L_{T1}(m)) + (L_{C0}(m)-L_{C1}(m))\big] \\ +\phi_{T1}-\phi_{T0}+\phi_{T1}^{CT}(m)-\phi_{T0}^{CT}(m)\end{aligned} \tag{4}$$

In [23] it was shown that the variation of $(\delta_{T0}(m)-\delta_{T1}(m))$ and $(L_{C0}(m)-L_{C1}(m))$ with N and $\frac{\partial N}{\partial h}$ (that is, with time) can be neglected compared to the variation of $(L_{T0}(m)-L_{T1}(m))$ with N and $\frac{\partial N}{\partial h}$. Then, the dependence with m of those terms can be dropped and the phase difference, $\Delta\Phi_{T0,T1}(m)$, is well approximated by:

$$\begin{aligned}\Delta\Phi_{T0,T1}(m) = -\frac{2\pi}{c} f_{LO}(k_{T1}-k_{T0})2\Delta R' + \\ \frac{2\pi(f_c+f_{L0})}{c}\big[(\delta_{T0}-\delta_{T1})+(L_{C0}-L_{C1})\big] \\ +\phi_{T1}-\phi_{T0}+\phi_{T1}^{CT}(m)-\phi_{T0}^{CT}(m) \\ +\frac{2\pi}{c}(f_c+f_{L0})(R_{T0}-R_{T1})\overline{N}(m)\cdot 10^{-6} + \\ \frac{2\pi}{c}(f_c+f_{L0})\big[\frac{h_{T0}-h_R}{2}R_{T0}-\frac{h_{T1}-h_R}{2}R_{T1}\big]\frac{\partial N(m)}{\partial h}\cdot 10^{-9}\end{aligned} \tag{5}$$

Therefore, the phase difference change, $\Delta\Phi_{T0,T1}(m_1,m_2)$, is given by:

$$\begin{aligned}\Delta\Phi_{T0,T1}(m_1,m_2) = \Delta\Phi_{T0,T1}(m_2)-\Delta\Phi_{T0,T1}(m_1) = \\ \frac{2\pi}{c}(f_c+f_{L0})(R_{T0}-R_{T1})\Delta\overline{N}\cdot 10^{-6} + \\ \frac{2\pi}{c}(f_c+f_{L0})\big[\frac{h_{T0}-h_R}{2}R_{T0}-\frac{h_{T1}-h_R}{2}R_{T1}\big]\Delta\frac{\partial N}{\partial h}\cdot 10^{-9} + \\ \phi_{T1}^{CT}(m_2)-\phi_{T0}^{CT}(m_2)-\phi_{T1}^{CT}(m_1)+\phi_{T0}^{CT}(m_1)\end{aligned} \tag{6}$$

which shows how the phase difference change relates to both, the change of the refractivity at the radar height, $\Delta\overline{N} = \overline{N}(m_2)-\overline{N}(m_1)$, and the change of the gradient of the refractivity, $\Delta\frac{\partial N}{\partial h} = \frac{\partial N}{\partial h}(m_2)-\frac{\partial N}{\partial h}(m_1)$, [19].

Clearly, to obtain the refractivity change, either the change of the gradient of the refractivity is obtained by any other means or it has to be jointly estimated with the refractivity change. This last approach was the one considered in [19]. A linear least squares approach was used to estimate the change of the refractivity and the change of the refractivity gradient from measurements of the phase difference change from several pairs of stationary targets. Changes of the refractivity and of the refractivity gradient were obtained from the phase difference change between consecutive pulses to minimize the probability of wrapping. The higher probability of wrapping in hilly areas prevented the obtaining of the change of the refractivity and the refractivity gradient from the phase difference variation between the current received pulse and a former received pulse at known tropospheric conditions. Then, to obtain absolute values of the refractivity and of the refractivity gradient, consecutively measured changes of the refractivity and its gradient were accumulated from a first reference pulse for which the refractivity and the refractivity gradient were known. As in the case of "strictly flat earth", accumulating consecutive estimates of the changes of the refractivity and its gradient caused a continuous increase of the variance of the refractivity as well as of the variance of the refractivity gradient estimates. To keep the error of the estimates within reasonable values, frequent recalibration of the system was required. Avoiding the need for frequent recalibration has been one of the objectives during the development of the method proposed in this paper, which is based on a non-linear least squares approach.

III. Estimation of the Refractivity and its Gradient: A Non-linear Least Squares Based Approach

The approach to be derived in the following is based on the expression for the phase of received signals given in Equation (1). To obtain that expression a constant refractivity gradient in the lower part of the troposphere was assumed. Therefore, the following approach will provide estimates of the refractivity at the radar height and of the refractivity gradient assuming it does not vary with height.

Let us consider K pairs of stationary targets. $\Delta\Phi_{T0_k,T1_k}(m)$ is the phase difference measured for the m-th transmitted pulse corresponding to the k-th target pair. Let us denote by $\Delta\Phi_{T0_k,T1_k}(\overline{N},\frac{\partial N}{\partial h})$ the phase difference for that target pair as a function of $\overline{N}$ and $\frac{\partial N}{\partial h}$ under clutter free conditions. The values of the refractivity and of the refractivity gradient, at the time the m-th pulse is transmitted, can be estimated using a least squares based approach. Obtaining of $\overline{N}$ and $\frac{\partial N}{\partial h}$ from minimizing the sum of squares of residuals,

$$\sum_{k=1}^{K}\Big[\angle\Big(e^{j\Delta\Phi_{T0_k,T1_k}(\overline{N'},\frac{\partial N'}{\partial h})}\cdot e^{-j\Delta\Phi_{T0_k,T1_k}(m)}\Big)\Big]^2$$

may lead to large errors in noisy situations due to the "periodicities" of the sum of squares of residuals. To avoid this, $\overline{N}$ and $\frac{\partial N}{\partial h}$ are obtained from minimizing the weighted sum of the sum of squares of residuals and a function of the variation of the refractivity and of the refractivity gradient from the previous measurement, $f(\Delta\overline{N},\Delta\partial N/\partial h)$:

$$\begin{aligned}\overline{N},\frac{\partial N}{\partial h} = \arg\min_{\overline{N'},\frac{\partial N'}{\partial h}}\Bigg(w_a\cdot\sum_{k=1}^{K}\Big[\angle\Big(e^{j\Delta\Phi_{T0_k,T1_k}(\overline{N'},\frac{\partial N'}{\partial h})} \\ \cdot e^{-j\Delta\Phi_{T0_k,T1_k}(m)}\Big)\Big]^2 + (1-w_a)\cdot f(\Delta\overline{N'},\Delta\partial N'/\partial h)\Bigg)\end{aligned} \tag{7}$$

$\Delta\Phi_{T0_k,T1_k}(\overline{N}, \frac{\partial N}{\partial h})$ is readily obtained from Equation (5):

$$\Delta\Phi_{T0_k,T1_k}(\overline{N}, \tfrac{\partial N}{\partial h}) = A_k + B_k\overline{N} + C_k \tfrac{\partial N}{\partial h} \quad (8)$$

with:

$$A_k = -\frac{2\pi}{c} f_{LO}\left[(k_{T1_k} - k_{T0_k})2\Delta R'\right] + \frac{2\pi}{c}(f_c + f_{LO}) \cdot \left[(\delta_{T0_k} - \delta_{T1_k}) + (L_{C0_k} - L_{C1_k})\right] + \phi_{T1_k} - \phi_{T0_k}$$

$$B_k = \frac{2\pi}{c}(f_c + f_{LO})(R_{T0_k} - R_{T1_k}) \cdot 10^{-6}$$

$$C_k = \frac{2\pi}{c}(f_c + f_{LO})(\frac{h_{T0_k} - h_R}{2} R_{T0_k} - \frac{h_{T1_k} - h_R}{2} \cdot R_{T1_k}) \cdot 10^{-9}$$

A_k, B_k and C_k are unknown since the range to the stationary targets, R_{T0_k}, R_{T1_k}, their heights h_{T0_k}, h_{T1_k} and the backscatter phase of the stationary targets, ϕ_{T0_k}, ϕ_{T1_k} are unknown.

To obtain estimates of A_k, B_k and C_k and therefore, the phase difference function corresponding to each pair of stationary targets, the refractivity, as well as its gradient are modelled as random processes. Let us define the event $H : (\overline{N}_1 < \overline{N} < \overline{N}_2, (\partial N/\partial h)_1 < \partial N/\partial h < (\partial N/\partial h)_2)$ such that, the range of values of the phase difference, $\Delta\Phi_{T0_k,T1_k}(\overline{N}, \frac{\partial N}{\partial h})$ for values of $\overline{N}$ and $\partial N/\partial h$ within such event H, is within an interval of length 2π. In this case, the expected value of the phase difference of each target pair $(T0_k, T1_k)$ given the event H is well approximated by:

$$\boldsymbol{E}\left\{\Delta\Phi_{T0_k,T1_k}/H\right\} = A_k + B_k \cdot \overline{N}_H + C_k \frac{\partial N_H}{\partial h} \quad (9)$$

where $\overline{N}_H = \boldsymbol{E}\left\{\overline{N}/H\right\}$ is the mean value of the mean refractivity given H, $\frac{\partial N_H}{\partial h} = \boldsymbol{E}\left\{\frac{\partial N}{\partial h}/H\right\}$ is the mean value of the refractivity gradient given the same event H.

Now, $\boldsymbol{E}\left\{\Delta\Phi_{T0_k,T1_k}/H\right\}$ can be estimated from measurements of the phase difference if simultaneous measurements of the mean refractivity, $\overline{N}$ and its gradient, $\partial N/\partial h$ are available. The sample circular mean of all phase measurements taken at a time at which according to the alternative measurement method the refractivity and its gradient belong to the event H, is calculated to get an estimate of $\boldsymbol{E}\left\{\Delta\Phi_{T0_k,T1_k}/H\right\}$. It is of interest to remind here that though phase difference measurements are noisy due to the clutter, the expected value of this noise, as discussed in the Appendix, is zero. At the same time, the refractivity and refractivity gradient values corresponding to the event H, are averaged to obtain the estimates of $\overline{N}_H$ and $\frac{\partial N_H}{\partial h}$.

Then, calculating the expected value of the phase difference for several events H allows obtaining estimates of A_k, B_k and C_k by linear least squares, that is, allows obtaining an estimate of the phase difference function $\Delta\Phi_{T0_k,T1_k}(\overline{N}, \frac{\partial N}{\partial h})$.

To this point a coherent transmitter has been assumed, that is, neither f_c nor f_{LO} change with time. This is not the case if magnetron transmitters are considered. In this case, the magnetron frequency changes with time and the local oscillator frequency is set up to follow the frequency of the magnetron. Let us consider that the magnetron frequency has varied Δf Hz w.r.t. f_c and analogously, the local oscillator frequency has varied Δf Hz w.r.t. f_{LO}. Now the phase difference between targets $T0_k$ and $T1_k$ is a linear function of $\overline{N}$, $\frac{\partial N}{\partial h}$ and Δf, as:

$$\Delta\Phi_{T0_k,T1_k}(\overline{N}, \tfrac{\partial N}{\partial h}, \Delta f) = A_k + B_k\overline{N} + C_k \tfrac{\partial N}{\partial h} + D_k\Delta f \quad (10)$$

with:

$$D_k = -\frac{2\pi}{c}\left[(k_{T1_k} - k_{T0_k})2\Delta R'\right] + \frac{4\pi}{c}\left[(\delta_{T0_k} - \delta_{T1_k}) + (L_{C0_k} - L_{C1_k})\right]$$

Consequently, measuring $\Delta\Phi_{T0_k,T1_k}(\overline{N}, \frac{\partial N}{\partial h}, \Delta f)$ in this case requires to generalize the definition of the event H as $H : (\overline{N}_1 < \overline{N} < \overline{N}_2, (\partial N/\partial h)_1 < \partial N/\partial h < (\partial N/\partial h)_2), \Delta f_1 < \Delta f < \Delta f_2$. Then, as for the coherent transmitters, definition of enough events allows linear least squares estimation of A_k, B_k, C_k and D_k, that is, of the phase difference function.

Once the phase difference function has been determined for all target pairs, the refractivity and the refractivity gradient can be estimated from phase radar measurements by the least squares based approach defined in Equation (7).

IV. Algorithm Implementation

To implement the algorithm to estimate the refractivity and its gradient it is necessary to identify and pair the stationary targets within the radar coverage area and to find the phase difference function $\Delta\Phi_{T0_k,T1_k}(\overline{N}, \frac{\partial N}{\partial h})$ for all pairs of targets. Estimation of the phase difference function is based on averaging as many measurements as possible in order to average out measurement errors as well as the noise due to clutter. The technique presented in this paper is different to previous approaches that do not consider the estimation of the phase difference function, but just the estimation of the value of the phase difference function for a known value of the refractivity. For that, those methods looked for a period of time, relatively short, a few hours at most, during which refractivity conditions in the atmosphere could be considered stable in time and spatially homogeneous. Though data need to be recorded only for some hours, determining such period of time with stationary conditions may require observation of the troposphere conditions for a much longer time. For the calibration proposed here, backscattered data for several days to several weeks, depending on the type of the transmitter and the number of scans per day, are required. However, it is important to point out that recording of the calibration data does not affect the radar operation. Once the scanning strategy of the radar has been defined, including a low elevation scanning for refractivity estimation, the radar operation is not changed for calibration. During the first days or weeks, the data obtained at each low elevation scanning are just recorded, no refractivity estimations are produced. This recorded data are used for the calibration. Once the calibration is performed refractivity and refractivity gradient estimates are produced after each low elevation scan.

With all data recorded, the first step is to identify the stationary targets. Identification of stationary targets has been addressed in [6], [12], [21]. In all cases the objective was to identify, from radar measurements, the ground targets that

remained unchanged with time. The difficulty encountered by all methods is that the effects of target movements and atmospheric refractivity changes on the radar signal cannot be separated. All methods consider that refractivity changes are slow with time, so the intensity and phase of the backscattered pulses, within a scan, from a stationary target should remain practically invariant. Considering this, and the large number of scans available at the calibration stage, the following stationarity index, SI, has been defined:

$$SI = \frac{1}{K(K-1)/2} \sum_{k \neq l} \frac{\sum e^{j(\phi_{kn} - \phi_{ln})}}{N} \tag{11}$$

where ϕ_{kn} is the phase of the n-th pulse of the k-th scan. N consecutive pulses at each scan and K scans randomly chosen are used. All targets whose SI is over a predefined threshold, set up at a conservative 0.95, are considered stationary.

Now, to pair the stationary targets, the events $H : (\overline{N}_1 < \overline{N} < \overline{N}_2, (\partial N/\partial h)_1 < \partial N/\partial h < (\partial N/\partial h)_2), \Delta f_1 < \Delta f < \Delta f_2)$, for the general case of a magnetron transmitter, need to be defined. The stationary targets are paired verifying that the two targets of a pair are in the same azimuth direction and that its phase difference change for the maximum refractivity and refractivity gradient changes within each one of the defined events H does not wrap. There is a trade-off here. If the events H have been defined too wide, the maximum distance between the stationary targets of a pair has to be reduced to avoid wrapping, if the events H are too narrow, the maximum distance between the stationary targets of a pair can be higher and more pairs would be available, but the time to obtain enough samples for each event will be longer, and consequently, the time required for the calibration.

To perform the calibration, that is to obtain the phase difference function for all pairs of stationary targets, refractivity and refractivity gradient data for the period of time during which radar data were recorded, are required. These refractivity and refractivity gradient data have to be obtained by an alternative measurement method in the radar area as, for example, automatic weather stations within the radar coverage area. Alternatively, ERA5 reanalysis data provided by the European Centre for Medium-Range Weather Forecasts (ECMWF) may be used, such as in [24] [25]. ERA5 data have a temporal resolution of 1 hour, a spatial resolution of 30 km and resolve the atmosphere using 137 levels that extend from the surface up to 80 km. The refractivity and its gradient can be calculated from the temperature, the humidity and the geopotential height data. In any case, the refractivity and refractivity gradient measurements obtained allow to determine the phase difference measurements corresponding to a given event so that, the sample circular mean estimator is used to compute the expected value of the phase difference for each event H, $\boldsymbol{E}\{\Delta\Phi_{T0_k,T1_k}/H\}$ and for each pair of targets. At the same time, the sample mean of the refractivity and of the refractivity gradient measurements corresponding to each event H provides estimates of $\overline{N}_H$ and $\partial N_H/\partial h$. It is during these averaging steps, that it is expected to average out the measurement errors, not only of the radar phase measurements but also of the refractivity and refractivity gradient measurements obtained by an alternative method.

Now, from the estimated values of $\boldsymbol{E}\{\Delta\Phi_{T0_k,T1_k}/H\}$, $\overline{N}_H$ and $\partial N_H/\partial h$ for several events H, the phase difference function for all pairs of stationary targets is obtained using linear least squares estimation. Just events H with a large number of samples are considered. Finally, a residue analysis is performed. Those pairs of targets with a large standard deviation of the residues are discarded.

At this point, the real-time estimation of the refractivity and its gradient starts. The phase from all stationary targets and the local oscillator frequency are read. Then the phase difference is calculated for all previously selected pairs of targets. Finally, using the phase difference function calculated in the calibration stage, estimates of the absolute refractivity and of the absolute refractivity gradient are obtained by means of Equation (7).

V. Results

Data from different radars at different locations have been used to evaluate the refractivity estimation algorithm. Data collected during the International H_2O project 2002 (IHOP_2002) [26], that took place in the Southern Great Plains of the United States from May 13, 2002 to June 25, 2002, remain open access. These data have been used for the initial validation of the algorithm. The NCAR/EOL's S-Pol radar [27] was used during this project. This radar operates at S-band with a klystron based transmitter. Additionally, the Portuguese Institute for Sea and Atmosphere (IPMA, Instituto Português do Mar e da Atmosfera) and the Regional Meteorological Agency of Galicia, Spain (Meteogalicia) have collected data with their radars. IPMA collected data with two radars located at Arouca and Coruche respectively. Meteogalicia collected data with its radar located at Cuntis. These radars are located in the west coast of the Iberian Peninsula. The radar operated by Meteogalicia at Cuntis has collected data for different periods of time since July 19, 2019. The radar operated by IPMA at Arouca started to collect data on August 6, 2019, the one at Coruche started to collect data on July 15, 2021. In all cases radar phase measurements were taken every five minutes. All these radars work at C-band with magnetron-based transmitters. The radar configurations for the phase measurements are summarized in Table III.

TABLE III
Radar parameters used during the phase measurements.

Parameter	NCAR/EOL's S-POL	Arouca	Coruche	Cuntis
Height (amsl)	875m	1097m	193m	762m
Frequency	2.8 GHz	5.63 GHz	5.64 GHz	5.6 GHz
Beam Width	0.918º	0.95º	0.95º	0.95º
PRF	1200 Hz	890 Hz	890 Hz	890 Hz
Scan Rate	10 º/s	18 º/s	18 º/s	18 º/s
Pulse Duration	1μs	1μs	0.88μs	1μs
Range Resolution	150 m	150 m	125 m	150 m
Scan Elevation Angle	0º	-0.1º	0.1º	-0.5º

ERA5 data have been used to calculate the mean refractivity at the radar height and its gradient at the calibration step of the algorithm. ERA5 data are available for all radars and for the entire time that data were being recorded. For the NCAR/EOL's S-Pol radar, during IHOP_2002 project and for

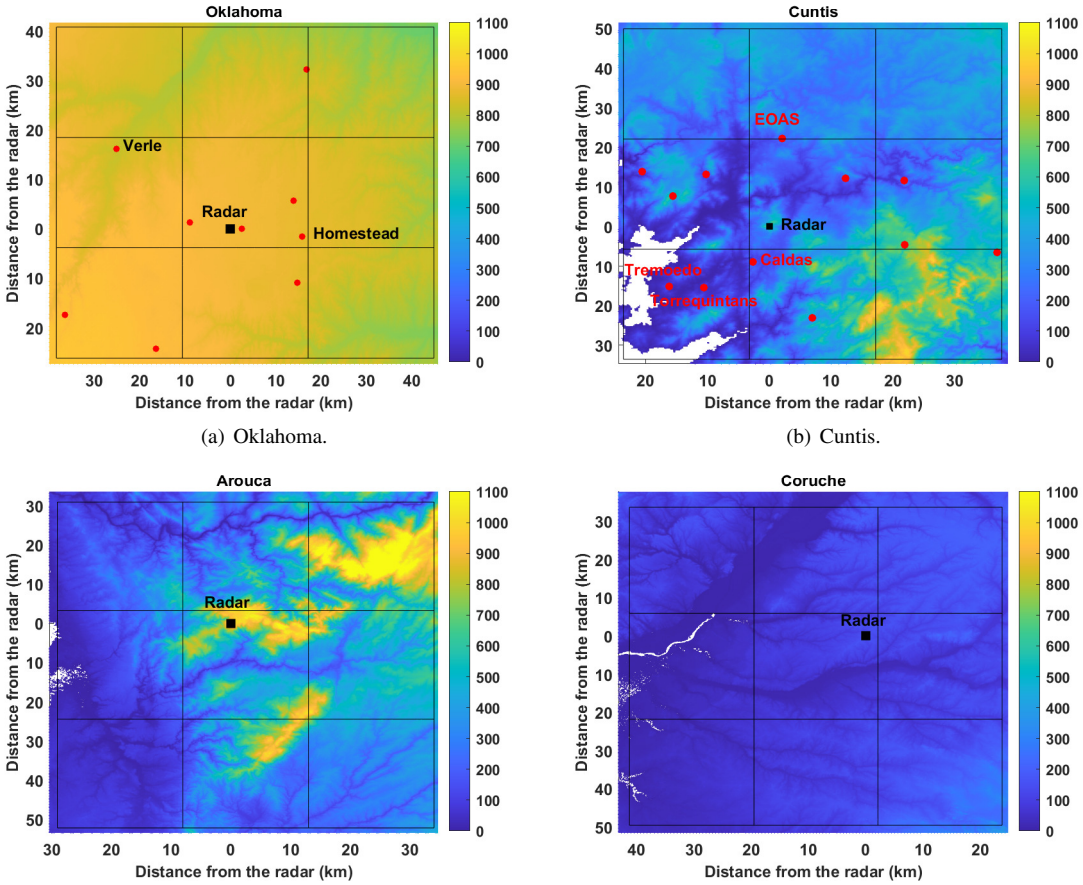

(a) Oklahoma. (b) Cuntis.

(c) Arouca. (d) Coruche.

Fig. 1. Maps of the terrain around each radar. Radar location is shown. Black grid shows the ERA5 cells used for calibration.

the Meteogalicia radar at Cuntis there are also weather station data that can be used for calibration. However, it was preferred to calibrate all radar data using the same data source and, where refractivity data from other sources were available, to use them for further evaluation and discussion of the results. Figure 1 shows the map of the terrain height and the limits of the ERA5 cells used to calculate the refractivity data needed for the calibration at each radar: the refractivity at the radar height and the refractivity gradient. Lowest ERA5 levels, up to the radar height, are used to estimate the refractivity and refractivity gradient. Regarding the terrain orography, the areas around the radars at Oklahoma and Coruche are relatively flat, with height differences between the radar and the stationary ground targets identified around 100 m or less. Around Cuntis and Arouca radar, the terrain is much hillier, with height differences between the radar and the stationary ground targets up to 1000 m.

Regarding the identification of the stationary targets, in the case of the radars at Cuntis, Arouca and Coruche, the stationarity index defined in Equation (11) was considered. In the case of the NCAR/EOL's S-Pol radar at Oklahoma, only phase data, already integrated, were available. Consequently, the reliability index defined in [6] was used to identify the stationary targets. In all cases, after the stationary targets were identified, they were paired. For that, the events H for the calibration had to be defined. In the case of the NCAR/EOL's S-Pol radar at Oklahoma the events defined were of 10 N-units length in refractivity and of 30 N-units/km length in refractivity gradient. For the Meteogalicia radar at Cuntis and the IPMA radars at Arouca and Coruche, with magnetron-based transmitters the events were of 10 N-units length in refractivity, 20 N-units/km length in refractivity gradient and 100 kHz length in LO frequency variation. For Meteogalicia and IPMA radars, the events were defined smaller since the phase difference wraps faster due to the higher height differences between the radars and the stationary targets. In all cases, those pairs of targets, whose phase difference wraps for refractivity and refractivity gradient variations within an event, are discarded. To estimate the phase difference between the stationary targets of a pair, the height of each target is estimated as the mean height of the terrain at the range gate where the target is located and the range of each target is estimated as the distance to the range gate center. Estimates of the mean refractivity at the radar height and of the refractivity gradient for the four radars are now presented.

A. Mean refractivity at the radar height for a klystron-based radar

Figure 2 shows the radar refractivity estimates obtained from measurements with the NCAR/EOL's S-Pol radar at

Oklahoma [28].

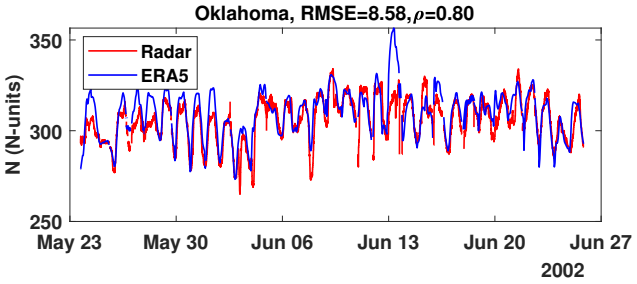

Fig. 2. Radar and ERA5 refractivity estimates. NCAR/EOL's S-Pol radar data were used. Radar refractivity is calculated at the radar height (875 m amsl). Radar refractivity are field estimates up to 45 km range.

Radar refractivity and ERA5 refractivity estimates at the radar height are shown. Radar refractivity estimates are field estimates up to 45 km range, and no time averaging is performed. Within the coverage area of the radar, up to 45 km, 8968 stationary target pairs were identified. ERA5 refractivity estimates are obtained from the values of refractivity at the ERA5 cells depicted in Figure 1a using linear regression. Radar data from May 11, 2002 to May 23, 2002, up to 3000 scans, have been used for calibration. The results shown correspond to radar data scans obtained after the scans used for calibration, from May 23, 2002, to the end of the IHOP_2002 project, in June 25, 2002. The root mean square error (RMSE) between the radar and the ERA5 refractivity estimates is 8.58 and their correlation coefficient (ρ) is 0.8. It can be observed that for some periods of time, e.g. during May 24, May 28 or June 13, ERA5 refractivity estimates are significantly higher than radar refractivity estimates. However, these high values of the refractivity (e.g. on June 13) shown by ERA5 data are not shown by the radar data or by the WS around the radar as can be seen in Figure 3, which shows radar refractivity estimates versus WS measurements at Homestead and Verle, respectively [29]. These WS (see Figure 1a) are located at a height very close to the radar height, Verle height is 862 m, Homestead height is 862 m and the radar height is 875 m. Verle is approximately 30 km west of the radar while Homestead is approximately 15 km east of the radar. Radar refractivity estimates at Homestead and Verle are obtained considering only those pairs of stationary targets within an area of 8×10 km^2 centered at the weather stations, 285 target pairs were found for Homestead and 153 for Verle. The agreement between radar refractivity estimates and WS measurements at Homestead (RMSE=4.75, $\rho = 0.94$) and Verle (RMSE=4.1, $\rho = 0.97$) is very good, despite the fact that ERA5 data were used for the calibration.

B. Mean refractivity at the radar height for a magnetron-based radar

Figure 4 shows radar refractivity estimates at the radar height obtained with the C-band, magnetron-based radar operated by Meteogalicia at Cuntis in a hilly area. Within the coverage area of the radar, up to 60 km in range, 1003 target pairs were identified. ERA5 refractivity data at the radar height

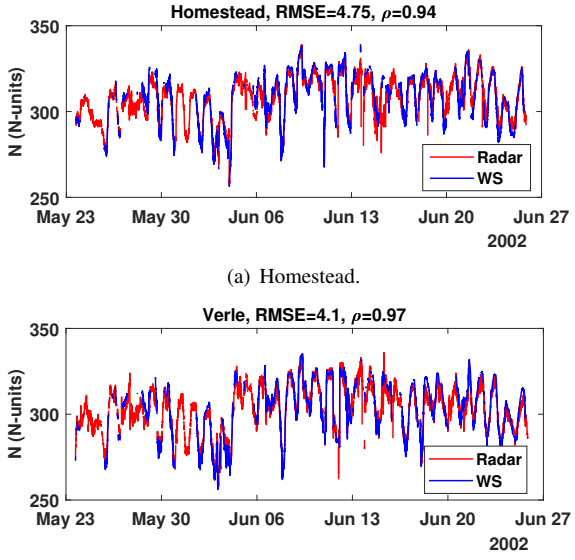

(a) Homestead.

(b) Verle.

Fig. 3. Radar and WS refractivity estimates at Oklahoma. NCAR/EOL's S-Pol radar data were used. Radar refractivity is calculated over an area of about 8×10 km^2 at WS height: (a) Homestead (862 m amsl); (b) Verle (862 m amsl).

are also shown. A total of 10000 scans, recorded between July 19, 2019 and September 29, 2019, have been used for the calibration. The radar refractivity estimates shown in the figure have been obtained from radar data recorded along the summer of 2020, one year after the calibration was performed. Good agreement was found between radar and ERA5 refractivity estimates, with a RMSE of 5.16 and a correlation coefficient $\rho = 0.88$.

Radar refractivity estimates for smaller areas are shown in Figure 5. The first area (8×8 km^2, 149 target pairs) is around the EOAS WS, 22 km north of the radar, the second area (15×15 km^2, 76 target pairs), with two weather stations, Torrequintans and Tremoedo, is located between 20 and 30 km southeast from the radar and the third area (15×15 km^2, 781 target pairs) is around the Caldas WS 10 km southeast from the radar. Figures show radar refractivity estimates at the height of the weather stations, EOAS WS is at 255 m amsl, Torrequintans at 52 m amsl, Tremoedo at 72 m amsl and Caldas at 268 m amsl. The areas have been defined to include a sufficient number of stationary targets. The agreement between radar refractivity estimates and WS data is very good (see Table IV and Table V). Results in Torrequintans/Tremoedo are noisier, probably because despite the size of the area, the number of stationary targets is the lower. Increasing the area size to include more stationary targets would reduce the noise of the estimates, but the comparison of the radar refractivity estimates with the point measurements provided by WS would be less meaningful.

Radar refractivity estimates obtained with Coruche and Arouca radar data are shown in Figure 6. These radars, operated by IPMA, are C-band magnetron-based radars. Within the coverage area of these radars 1600 and 1057 target pairs were identified, respectively.The Arouca data time series is the

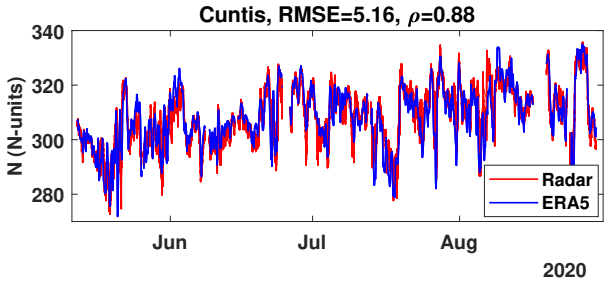

Fig. 4. Radar and ERA5 refractivity estimates. Cuntis radar data were used. Radar refractivity are field estimates up to 60 km range at radar height (762 m amsl).

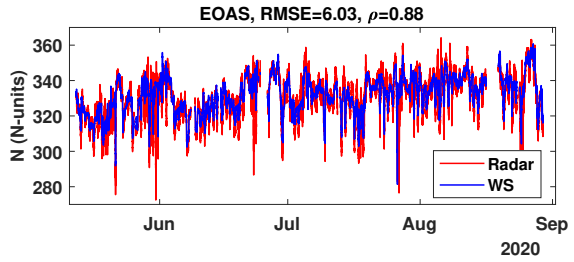

(a) EOAS.

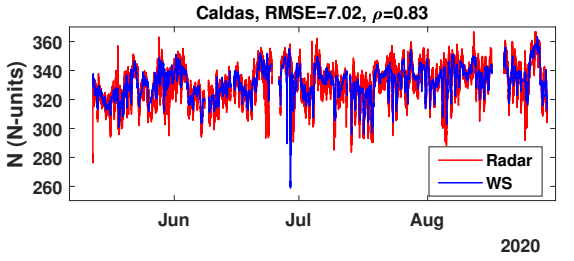

(b) Caldas.

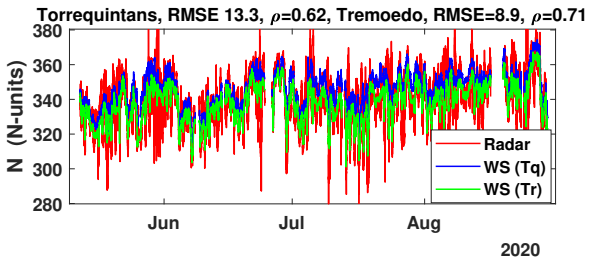

(c) Torrequintans and Tremoedo.

Fig. 5. Radar and WS refractivity estimates. Cuntis radar data were used. Radar refractivity is calculated at WS height: (a) EOAS (255 m amsl) over an area of about 8×8 km^2; (b) Caldas (268 m amsl) over an area of about 15×15 km^2; (c) Torrequintans (52 m amsl) and Tremoedo (72 m amsl) over an area of about 15×15 km^2.

longest. Estimates are shown for almost the whole 2021 year. Calibration was performed with data recorded previously.

C. Refractivity gradient

The refractivity gradient is jointly estimated with the refractivity. RMSE and correlation coefficients are calculated using all estimates while in Figure 7 only part of the time series of refractivity gradient estimates from radar data and ERA5 data are shown so that the diurnal variations can be

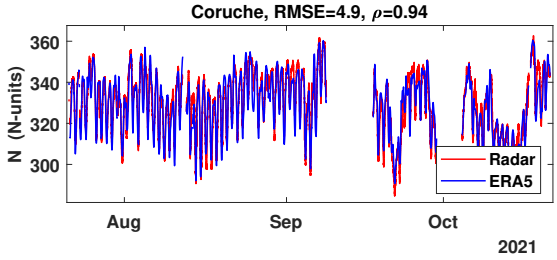

(a) Coruche.

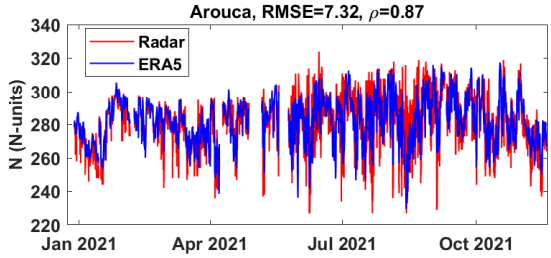

(b) Arouca.

Fig. 6. Radar and ERA5 refractivity estimates. Radar refractivity are field estimates up to 60 km range at radar height: (a) Coruche radar (193 m amsl) data were used; (b) Arouca radar (1097 m amsl) data were used.

appreciated. Estimates of the refractivity gradient are very noisy, so just field estimates of radar refractivity gradient have been considered. That is, data from all stationary targets within the coverage area of the radarare used to obtain a refractivity gradient estimate. This is in agreement with the tropospheric refractivity model assumed for the theoretical modelling of the radar phase. This model considers that the tropospheric refractivity gradient variations with distance from the radar can be neglected for the considered radar coverage areas. As expected (see Figure 8) , the accuracy of the refractivity gradient estimates is worse in flat areas as Oklahoma and Coruche, than in hilly areas as Cuntis and Arouca with significantly higher height differences between the radar and the stationary targets. Particularly, in Oklahoma, though refractivity gradient estimates follow the diurnal variations, they present large biases at high superrefractive conditions. The reduced accuracy of the refractivity gradient estimates at Oklahoma is due to the small height differences between the stationary targets and the radar.

Tables IV and V summarize the achieved results in the different areas for both the mean refractivity and the refractivity gradient estimates.

VI. Conclusions

A non-linear least squares approach was used to present and analyze a novel method for estimating tropospheric refractivity from radar phase observations. The proposed technique allows the joint and simultaneous estimation of the radio refractivity and its vertical gradient in the lower part of the atmosphere. Therefore, it works in both flat and hilly areas. It operates in the S- and C-band frequencies and can be used in radars with magnetron or klystron-based transmitters. Important properties of the method presented are that estimates of the refractivity and its gradient are not cumulative, so their variance does not

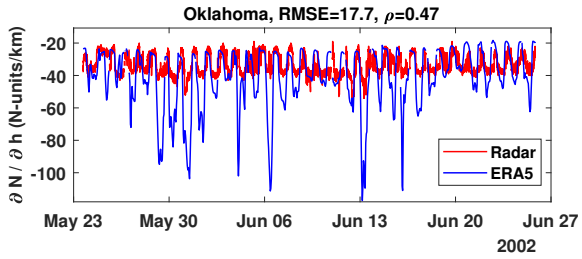

(a) Oklahoma.

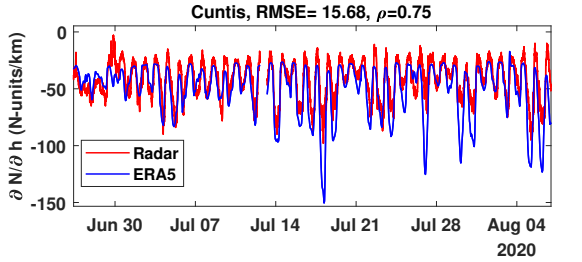

(b) Cuntis.

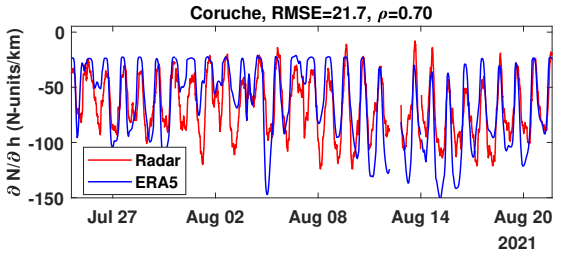

(c) Coruche.

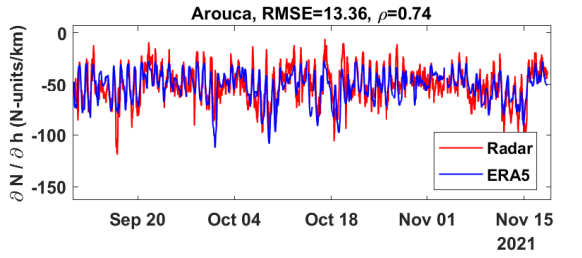

(d) Arouca.

Fig. 7. Radar and ERA5 refractivity gradient estimates. Radar refractivity gradient are field estimates: (a) Oklahoma; (b) Cuntis; (c) Coruche; (d) Arouca

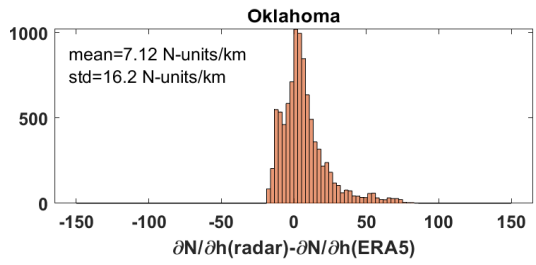

(a) Oklahoma.

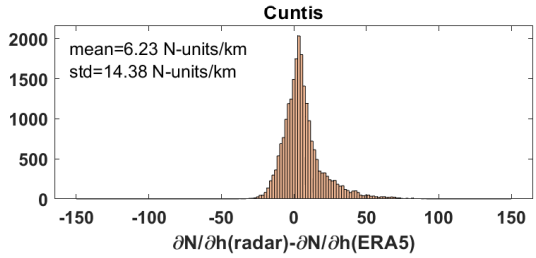

(b) Cuntis.

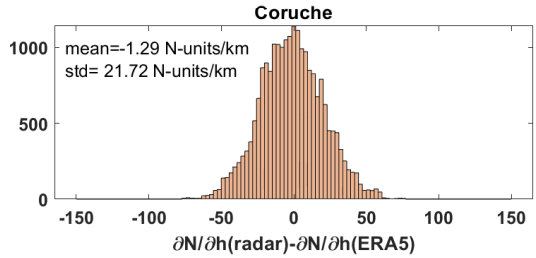

(c) Coruche.

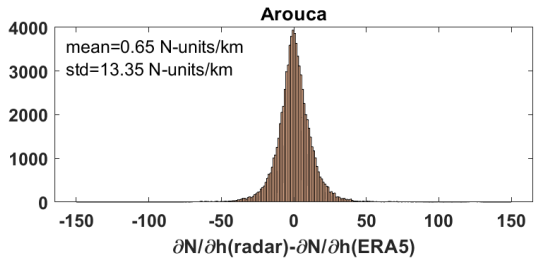

(d) Arouca.

Fig. 8. Histogram of radar minus ERA5 refractivity gradient estimates: (a) Oklahoma; (b) Cuntis; (c) Coruche; (d) Arouca

TABLE IV
SUMMARY OF THE REFRACTIVITY-RELATED EVALUATION RESULTS.

Radar	Area	Reference Source	RMSE	ρ	Bias
Oklahoma	45-km range area	ERA5	8.58	0.8	-3.52
Oklahoma	Homestead	WS (Homestead)	4.75	0.94	-1.74
Oklahoma	Verle	WS (Verle)	4.10	0.97	-1.34
Cuntis	60-km range area	ERA5	5.16	0.88	0.22
Cuntis	Caldas	WS (Caldas)	7.02	0.83	-1.42
Cuntis	EOAS	WS (EOAS)	6.03	0.88	-1.42
Cuntis	Tremoedo	WS (Tremoedo)	8.90	0.71	1.15
Cuntis	Torrequintans	WS (Torrequintans)	13.3	0.62	-6.29
Coruche	60-km range area	ERA5	4.90	0.94	0.68
Arouca	60-km range area	ERA5	7.32	0.87	0.32

TABLE V
SUMMARY OF THE GRADIENT-RELATED EVALUATION RESULTS.

Radar	Area	Reference Source	RMSE	ρ	Bias
Oklahoma	45-km range area	ERA5	17.7	0.47	7.10
Cuntis	60-km range area	ERA5	15.68	0.75	6.23
Coruche	60-km range area	ERA5	21.70	0.7	-1.29
Arouca	60-km range area	ERA5	13.36	0.74	0.86

increase with time, and the range of refractivity values that can be measured is not limited.

Refractivity and refractivity gradient estimates were derived using data from four different radars to validate the method for different systems and locations. The obtained estimates are in good agreement with the ECMWF ERA5 dataset as well as with data from local weather stations, but there are a few aspects that need to be explored and studied further in order to improve the performance of the presented technique.

The accuracy of the final estimates is heavily determined

by the quality of the observations. Hence, improving the identification of stationary targets within the coverage area should enhance the estimation performance. In addition, it is necessary to study how different stationary target pairing methods can expand the range of refractivity and refractivity gradient values for which the least squares function does not wrap.

The other determining factor in the performance of the algorithm is the calibration stage. The proposed calibration technique is based on the large amount of data that can be available, allowing the noise in the radar data as well as the noise in the calibration reference data to be averaged out. Consequently, the demands on the accuracy and precision of the reference data can be relaxed. On the other hand, due to the large amount of data required, starting to generate radar-based refractivity estimates might take several weeks. In any case, the calibration time is small in comparison to the radar operational life. Furthermore, while the results showed that the calibration is valid for long time spans, once the method is implemented in the radar, randomly selected scans can be recorded to increase the amount of data available for calibration, which can then be recalculated off-line without interrupting the radar routine.

Finally, it should be pointed out that the proposed method was designed without the need for any hardware additions or modifications in order to facilitate its actual implementation. Likewise, ERA5 data (with global coverage) were used for calibration to avoid the need for extra measurement equipment during the calibration process, although if data from other sensors are available they can also be used for calibration. That is, the proposed refractivity estimation procedure can be directly implemented on most radars within the European weather radar network to expand their utility without any additional requirements besides the actual radar hardware.

APPENDIX
RADAR RECEIVED SIGNAL PHASE MODEL

Obtaining the variation of the refractivity and its gradient from the changes they cause in the phase of the electromagnetic waves requires to know how the received signal phase at the radar relates to the tropospheric refractivity and its gradient. To this end, let us start considering the m-th transmitted pulse by the radar that is given by:

$$s_{TX}(t,m) = A \cdot e^{j(2\pi f_c t + \phi_{TX}(m))} \qquad 0 \le t \le T \tag{12}$$

with A the amplitude of the transmitted pulse, T the time length of the pulse, f_c the carrier or transmitter frequency and ϕ_{TX} the transmitter phase of the m-th pulse. For later discussions it is of interest to point here that the transmitter frequency, f_c, as well as the transmitter phase, ϕ_{TX}, may change from pulse to pulse.

As discussed in [11] and subsequent papers on the topic, for radar refractivity estimation, the signals of interest are those backscattered from stationary targets though the signal at the receiver input is due, not only to backscattering of the transmitted pulse by a stationary target, but also to backscattering from the terrain surrounding the stationary target within the same resolution radar cell (i.e. clutter). Let us consider a stationary target , $T0$, placed at a surface distance d_0 from the radar. Then, the received signal, the addition of the desired signal from the stationary target and the undesired signal from the clutter, can be expressed as:

$$r(t,m) = s_{TX}(t,m) \star (A_{CT}(t,m)e^{j\phi_{CT}(t,m)} + A_{T0}e^{j\phi_{T0}}\delta(t - t_{T0}(m))) \tag{13}$$

where the symbol $\star$ indicates convolution in t, $A_{CT}(t,m)e^{j\phi_{CT}(t,m)}$ represents the backscattering response of the clutter at the time the m-th pulse is transmitted and $A_{T0}e^{j\phi_{T0}}\delta(t - t_{T0(m)})$ the backscattering response of the stationary target at the same time. The time variable t is related to the distance travelled by the m-th pulse from the radar. In particular, $t_{T0}(m)$ is the time delay due to propagation, to and from the target $T0$ at the time the m-th pulse is transmitted. The backscattering coefficient of the surface clutter, $A_{CT}(t,m)e^{j\phi_{CT}(t,m)}$, can be modelled as a complex stochastic process, both in t and m. $A_{CT}(t,m)$ is the random amplitude and $\phi_{CT}(t,m)$ the random phase of the scattering coefficient. The stationary target $T0$ is characterized by a backscattering coefficient with constant amplitude and phase, $A_{T0}e^{j\phi_{T0}}$.

In [8], [9] it was shown that the phase of the received signal is determined not only by the transmitter frequency but also by the local oscillator frequency at the downconversion stage. Additionally, the receiver filter is considered here. Then, the received signal $r_{RX}(t)$ is given by:

$$r_{RX}(t,m) = (s_{TX}(t,m) \star (A_{CT}(t,m)e^{j\phi_{CT}(t,m)} + A_{T0}e^{j\phi_{T0}}\delta(t - t_{T0}(m)))) \cdot e^{-j(2\pi f_{LO}t)} \star h_{mf}(t) \tag{14}$$

where f_{LO} is the sum of all the frequencies of the different downconversion stages and $h_{mf}(t)$ is the receiver filter. The matched filter to the baseband transmitted pulse (in this case, a rectangular pulse of length T) has been considered.

Performing the convolutions, the contributions to the received signal due to both, the stationary target and the clutter are obtained. These two contributions are described below.

A. Contribution from the stationary point target T_0

The contribution of the stationary target $T0$ to the received signal, considering that the transmitter phase, ϕ_{TX}, is corrected for, is given by:

$$r_{RX}^{T0}(t,m) = A_{T0}^{R} \cdot e^{j(-2\pi f_c t_{T0}(m) + \phi_{T0})} \cdot e^{j2\pi(f_c - f_{LO})(\frac{t + t_{T0}(m)}{2})} \cdot \Delta(t - t_{T0}(m), T) \qquad -T \le (t - t_{T0}(m)) \le T \tag{15}$$

where A_{T0}^{R} and ϕ_{T0} are the signal amplitude and phase at the receiver output due to the stationary target and $\Delta(t,T)$ is the convolution of two rectangular pulses of length T.

B. Contribution from the clutter

To analyse the contribution of the clutter to the received signal, a simple model for the clutter is considered in this first approach. It is assumed that the clutter contribution results from adding the backscattered signal of many elemental scatterers (non statistically homogeneous) whose positions and

orientations vary independently with time (distance) and from pulse to pulse. The Central Limit Theorem applies and the clutter contribution at the receiver output can be modelled as a zero mean circularly symmetric complex Gaussian stochastic process in m. That is, the received signal due to the clutter is given by:

$$r_{RX}^{CT}(t,m) = A_{CT}^{R}(t,m) \cdot e^{j\phi_{CT}(t,m)} \tag{16}$$

where $A_{CT}^{R}(t,m)$ and $\phi_{CT}(t,m)$ are random variables that represent the amplitude and phase of the clutter signal at the receiver output; $\phi_{CT}(t,m)$ can be modelled as a uniform random variable.

C. Received radar phase

The received signal $r_{RX}(t)$, with contributions from the clutter and the stationary targets, Equation (14), is then sampled at kT':

$$\begin{aligned} &r_{RX}(kT',m) = \\ &\quad A_{T0}^{R} \cdot e^{j(-2\pi f_c t_{T0}(m) + \phi_{T0} + 2\pi(f_c - f_{LO})\left(\frac{kT' + t_{T0}(m)}{2}\right))} \\ &\cdot \Delta(kT' - t_{T0}(m), T) + A_{CT}^{R}(kT',m) \cdot e^{j\phi_{CT}(kT',m)} \end{aligned} \tag{17}$$

The received signal sample, corresponding to $k = k_{T0}$, where k_{T0} is the closest integer to t_{T0}/T', contains the contribution from the stationary target and a random contribution from the clutter. Considering that the clutter follows a zero mean circularly symmetric complex Gaussian distribution, the phase of this sample, for the m-th transmitted pulse, let us call it the target $T0$ phase $\Phi_{T0}(m)$, can be expressed as the sum of two terms, one that accounts for the travel time to the $T0$ target and a second one, $\phi_{T0}^{CT}(m)$ that accounts for the random contribution due to the clutter:

$$\begin{aligned} \Phi_{T0}(m) = &2\pi f_c \left(\frac{k_{T0}T'}{2} - \frac{t_{T0}(m)}{2}\right) + \phi_{T0} \\ &- 2\pi f_{LO} \left(\frac{k_{T0}T'}{2} + \frac{t_{T0}(m)}{2}\right) + \phi_{T0}^{CT}(m) \end{aligned} \tag{18}$$

The additive random contribution to the target $T0$ phase, $\phi_{T0}^{CT}(m)$, can be described as a zero mean random variable with a probability density function that depends on the stationary signal power to clutter signal power ratio, SNR, [30]:

$$\begin{aligned} f(\phi_{T0}^{CT}) = \frac{1}{2\pi}\Big[&e^{-SNR} + e^{-SNR\,sin^2(\phi_{T0}^{CT})}\sqrt{SNR}\sqrt{\pi} \\ &\cdot cos(\phi_{T0}^{CT})(1 - \mathrm{erf}(-\sqrt{SNR}\,cos(\phi_{T0}^{CT})))\Big] \end{aligned} \tag{19}$$

where $\mathrm{erf}(\cdot)$ stands for the error function. Now, let us focus on the time delay due to the two-way path to the target $t_{T0}(m)$ that determines the target $T0$ phase expected value. It varies with the refractivity conditions of the troposphere, in fact it is given by:

$$t_{T0}(m) = \frac{2}{c}\int_{C_{T0}} n(r,m)dr \tag{20}$$

with C_{T0} being the path that minimizes the integral and $n(r,m)$ the tropospheric index of refraction at path point r at the time the m-th pulse is transmitted. Assuming that the variation of the tropospheric index of refraction during the propagation time of the pulse, to and from the target is negligible and considering a spherically stratified troposphere where the index of refraction linearly decreases with height [20], $t_{T0}(m)$ can be expressed as [12], [19]:

$$\begin{aligned} t_{T0}(m) = \frac{2}{c}\Bigg(&R_{T0}(m)\left(\overline{n}(m) + \frac{h_{T0} - h_R}{2}\frac{\partial n(m)}{\partial h}\right) \\ &+ \frac{R_{T0}(m)(h_{T0} - h_R)^2 - R_{T0}^3(m)}{12a_e}\frac{\partial n(m)}{\partial h}\Bigg) \end{aligned} \tag{21}$$

where:

- $\overline{n}(m)$ is the mean refractive index at the radar height at the transmission of the m-th pulse.
- $\frac{\partial n(m)}{\partial h}$ is the gradient of the refractive index with respect to the height at the transmission of the m-th pulse.
- $R_{T0}(m)$ is the length of the ray path to the target, which for the applications of interest here may be up to a few tens of km. It depends on the refractivity gradient.
- h_{T0} is the target $T0$ height.
- a_e is the modified Earth's radius [20].

Now, considering $R_{T0}(m) = k_{T0}\Delta R' + \delta_{T0}(m)$, with:

- with $\Delta R'$ being defined as $cT'/2$ for convenience. This way, $k_{T0}\Delta R'$ is the distance to the center of the range gate considering free-space propagation
- $\delta_{T0}(m)$ being the distance between the target and the range gate center at the transmission of the m-th pulse. It varies with time depending on the refractive conditions, that is, it varies from pulse to pulse. Its maximum value is around half the radar range resolution, in the order of tens of meters.

Then, the target $T0$ phase can be expressed as:

$$\begin{aligned} \Phi_{T0}(m) = &-2\pi f_{LO}\left[\frac{k_{T0}2\Delta R'}{c}\right] + \phi_{T0} - 2\pi(f_c + f_{LO}) \\ &\cdot \left[\frac{\delta_{T0}(m)}{c} + \frac{L_{T0}(m)}{c} + \frac{L_{C0}(m)}{c}\right] + \phi_{T0}^{CT}(m) \end{aligned} \tag{22}$$

with $L_{T0}(m) = R_{T0}\left(\overline{N}(m)\cdot 10^{-6} + \frac{h_{T0}-h_R}{2}\frac{\partial N(m)}{\partial h}\cdot 10^{-9}\right)$ where, for convenience, the refractivity $N(r,m) = (n(r,m) - 1)\cdot 10^6$ and its gradient per km, $\partial N(m)/\partial h$, have been introduced, and $L_{C0}(m) = \frac{R_{T0}(h_{T0}-h_R)^2 - R_{T0}^3}{12a_e}\frac{\partial N(m)}{\partial h}\cdot 10^{-9}$

Data Availability

The ECMWF's ERA5 dataset is available at https://doi.org/10.24381/cds.bd0915c6. S-band radar data and related WS data were provided by NCAR/EOL under sponsorship of the National Science Foundation (website: http://data.eol.ucar.edu/). Data from the Cuntis, Arouca, and Coruche C-band radars, as well as related WS data, are stored on the servers of the research group. For data requests, please contact V. Santalla del Río at veronica@uvigo.es.

Acknowledgments

The authors would like to thank the ECMWF and NCAR/EOL for providing open access to the radar measurements and meteorological datasets used for this work.

REFERENCES

[1] E. R. Kursinski, G. A. Hajj, W. I. Bertiger, S. S. Leroy, T. K. Meehan, L. J. Romans, J. T. Schofield, D. J. McCleese, W. G. Melbourne, C. L. Thornton, T. P. Yunck, J. R. Eyre, and R. N. Nagatani, "Initial results of radio occultation observations of earth's atmosphere using the global positioning system," *Science*, vol. 271, pp. 1107–1110, 1996.

[2] J. Wickert, C. Reigber, G. Beyerle, R. König, C. Marquardt, T. Schmidt, L. Grunwaldt, R. Galas, T. Meehan, W. Melbourne, and K. Hocke, "Atmosphere sounding by gps radio occultation: First results from champ," *Geophys. Res. Lett.*, vol. 28, p. 3263–3266, 2001.

[3] F. Fabry, C. Frush, I. Zawadzki, and A. Kilambi, "On the extraction of near-surface index of refraction using radar phase measurements from ground targets," *Journal Atmospheric and Oceanic Technology.*, vol. 14, pp. 978–987, August 1997.

[4] T. M. Weckwerth, C. R. Pettet, F. Fabry, S. Park, M. A. LeMone, and J. W. Wilson, "Radar refractivity retrieval: validation and application to short-term forecasting," *Journal of Applied Meteorology.*, vol. 44, pp. 285–300, March 2005.

[5] R. D. Roberts, F. Fabry, P. C. Kennedy, E. Nelson, J. Wilson, N. Rehak, J. Fritz, V. Chandrasekar, J. Braun, J. Sun, S. Ellis, S. Reising, T. Crum, L. Money, R. Palmer, T. Weckwerth, and P. S., "REFRACTT_2006: Real-time retrieval of high-resolution low-level moisture fields from operational NEXRAD and research radars," *Bulletin American Meteorology Society.*, vol. 89, pp. 1535–1548, October 2008.

[6] B. L. Cheong, R. Palmer, C. D. Curtis, T. Y. Yu, D. S. Zrnic, and D. Forsyth, "Refractivity retrieval using the phased-array radar: First results and potencial for multimission operation," *IEEE Transactions on Geoscience and Remote Sensing.*, vol. 46, pp. 2527–2537, September 2008.

[7] D. Bodine, D. Michaud, R. D. Palmer, P. L. Heinselman, J. Brotzge, N. Gasperoni, B. L. Cheong, M. Xue, and J. Gao, "Understanding radar refractivity: Sources of uncertainty," *Journal of Applied Meteorology and Climatology.*, vol. 50, pp. 2543–2560, June 2011.

[8] J. Parent du Chatelet, C. Boudjabi, L. Besson, and C. O., "Errors caused by long-term drifts of magnetron frequencies for refractivity measurement with a radar: Theoretical formulation and initial validation," *Journal Atmospheric and Oceanic Technology.*, vol. 29, pp. 1428–1434, April 2012.

[9] J. C. Nicol, A. Illingworth, T. Darlington, and M. Kitchen, "Quantifying errors due to frequency changes and target location uncertainty for radar refractivity retrievals," *Journal Atmospheric and Oceanic Technology.*, vol. 30, pp. 2006–2024, April 2013.

[10] L. Besson, O. Caumont, L. Goulet, S. Bastin, L. Menut, E. Bresson, N. Fourrie, F. Fabry, and J. Parent du Chatelet, "Comparison of real-time refractivity measurements by radar with automatic weather stations, AROME-WMED and WRF forecast simulations during SOP1 of the HyMeX campaign," *Quarterly Journal of the Royal Meteorological Society.*, vol. 142, pp. 138–152, August 2016.

[11] F. Fabry, "Meteorological value of ground target measurements," *Journal Atmospheric and Oceanic Technology.*, vol. 21, pp. 560–573, April 2004.

[12] S. Park and F. Fabry, "Simulation and interpretation of the phase data used by radar refractivity retrieval algorithm," *Journal Atmospheric and Oceanic Technology.*, vol. 27, pp. 1286–1301, August 2010.

[13] P. L. Heinselman, B. Cheong, R. Palmer, D. Bodine, and K. Hondl, "Radar refractivity retrievals in oklahoma: Insights into operational benefits and limitations," *Weather Forecasting*, vol. 24, p. 1345–1361, 2009.

[14] J. Sun, "Convective-scale assimilation of radar data: progress and challenges." *Quarterly Journal of the Royal Meteorological Society.*, vol. 131, pp. 3439–3463, July 2005.

[15] K. Shimose, M. Xue, R. D. Palmer, J. Gao, B. L. Cheong, and D. J. Bodine, "Two-dimensional variational analysis of near-surface moisture from simulated radar refractivity-related phase change observations." *Adv. Atmos. Sci.*, vol. 30, pp. 291–305, 2013.

[16] N. A. Gasperoni, M. Xue, R. D. Palmer, and J. Gao, "Sensitivity of convective initiation prediction to near-surface moisture when assimilating radar refractivity: Impact tests using osses." *Journal of Atmospheric and Oceanic Technology.*, vol. 30, pp. 2281–2302, 10 2013.

[17] S. Park and F. Fabry, "Estimation of near-ground propagation conditions using radar ground echo coverage," *Journal Atmospheric and Oceanic Technology.*, vol. 28, pp. 165–180, February 2011.

[18] Y. Feng, F. Fabry, and W. T. M., "Improving radar refractivity retrieval by considering the change in the refractivity profile and the varying altitudes of ground targets," *Journal Atmospheric and Oceanic Technology.*, vol. 33, pp. 989–1004, May 2016.

[19] R. Nocelo and V. Santalla, "High temporal resolution refractivity retrieval from radar phase measurements," *Remote Sensing*, vol. 10(6), no. 6, p. 896, 2018.

[20] R. J. Doviak and D. S. Zrnic, "Doppler radar and weather observations," *Academy Press Inc., 2^{nd} Edition.*, vol. 1, p. 562pp., June 2006.

[21] J. C. Nicol and A. Illingworth, "The effect of phase-correlated returns and spatial smoothing on the accuracy of radar refractivity retrievals," *Journal Atmospheric and Oceanic Technology.*, vol. 30, pp. 22–39, January 2013.

[22] J. C. Nicol, A. Illingworth, and K. Bartholomew, "The potential of 1h refractivity changes from an operational c-band magnetron-based radar for numerical weather prediction validation and data assimilation," *Quarterly Journal of the Royal Meteorological Society.*, vol. 140, pp. 1209–1218, March 2014.

[23] R. Nocelo, "Estimation of the atmospheric refractivity from weather radar data," *PhD Thesis, 190pp, International Doctoral School, Universidade de Vigo, Spain*, 2018. [Online]. Available: http://hdl.handle.net/11093/993

[24] H. Hersbach, B. Bell, P. Berrisford, S. Hirahara, A. Horányi, J. Muñoz-Sabater, J. Nicolas, C. Peubey, R. Radu, D. Schepers, A. Simmons, C. Soci, S. Abdalla, X. Abellan, G. Balsamo, P. Bechtold, G. Biavati, J. Bidlot, M. Bonavita, G. De Chiara, P. Dahlgren, D. Dee, M. Diamantakis, R. Dragani, J. Flemming, R. Forbes, M. Fuentes, A. Geer, L. Haimberger, S. Healy, R. J. Hogan, E. Hólm, M. Janisková, S. Keeley, P. Laloyaux, P. Lopez, C. Lupu, G. Radnoti, P. de Rosnay, I. Rozum, F. Vamborg, S. Villaume, and J.-N. Thépaut, "The era5 global reanalysis," *Quarterly Journal of the Royal Meteorological Society*, vol. 146, no. 730, pp. 1999–2049, 2020.

[25] H. Hersbach, B. Bell, P. Berrisford, G. Biavati, A. Horányi, J. Muñoz Sabater, J. Nicolas, C. Peubey, R. Radu, I. Rozum, D. Schepers, A. Simmons, C. Soci, D. Dee, and J.-N. Thépaut, "ERA5 hourly data on pressure levels from 1979 to present," Copernicus Climate Change Service (C3S), Climate Data Store (CDS), Accessed: 2022-01-10, 2018, https://doi.org/10.24381/cds.bd0915c6.

[26] T. M. Weckwerth, D. B. Parson, S. E. Koch, J. A. Moore, M. A. LeMone, B. B. Demoz, C. Flamant, B. Geerts, J. Wang, and W. F. Feltz, "An overview of the international h2o project (ihop 2002) and some preliminary highlights," *Bulletin American Meteorology Society.*, vol. 85, pp. 253–277, February 2004.

[27] Earth-Observing-Laboratory, "S-band/ka-band dual polarization, dual wavelength doppler radar," *NCAR–UCAR*, 1996.

[28] UCAR/NCAR, "NCAR S-band Polarimetric (S-Pol) Data in cfRadial format. Version 1.0." Earth Observing Laboratory, Accessed: 2022-02-27, 2015, https://doi.org/10.5065/D65Q4TDJ.

[29] ——, "NCAR Supplemental Surface Met Station Data. Version 1.0." Earth Observing Laboratory, Accessed: 2019-11-22, 2008, https://data.eol.ucar.edu/dataset/77.053.

[30] N. Youssef, C.-X. Wang, M. Patzold, I. Jaafar, and S. Tabbane, "On the statistical properties of generalized rice multipath fading channels," in *2004 IEEE 59th Vehicular Technology Conference. VTC 2004-Spring (IEEE Cat. No.04CH37514)*, vol. 1, 2004, pp. 162–165.